

Monitoring of Sulfur Sites Doped in/on Titanium Oxide to Enable Photocatalysis under Visible Light Using S K-edge XANES

Yasuo Izumi*¹ and Yoshiyuki Shibata²

¹Department of Chemistry, Graduate School of Science, Chiba University,
1-33 Yayoi, Inage-ku, Chiba 263-8522

²Department of Nanomaterial Science, Graduate School of Advanced Integration Science, Chiba University,
1-33 Yayoi, Inage-ku, Chiba 263-8522

(Received June 9, 2009; CL-090549; E-mail: yizumi@faculty.chiba-u.jp)

The electronic state and site structure of doped S to enable photocatalysis of TiO₂ under visible light were investigated using S K-edge XANES compared to theoretically generated spectra. S sites substituting on the O atoms of TiO₂ were predominant and essential in photocatalysis based on S K absorption edge peak energy and post-edge pattern. Minor cationic/elemental S sites were detected as peaks due to the transition to vacant level of S3p, but most were lost during photocatalysis.

Photocatalysis has been investigated to decompose nitrogen oxides, sulfur oxides, and volatile organic compounds¹ and reduce water and carbon dioxide into hydrogen² and methanol/formic acid,³ respectively, over semiconductors, e.g., TiO₂. TiO₂ needs UV light to perform photocatalysis due to the band gap of 3.0–3.2 eV, but dopants effectively reduce the band gap to the visible light region.⁴

Electronic excitation from the valence band of TiO₂ to the impurity cationic V level and subsequent photoreduction over V–TiO₂ were monitored using V K-edge XAFS.^{5–7} Charge recombination occurs less frequently in anion-doped TiO₂. Doped anions effectively reduce the band gap and promote photooxidation under visible light.⁸ In this letter, the electronic structure of doped S sites in/on TiO₂ and the change during ethanol photooxidation were monitored using S K-edge XANES.

Two types of S-doped TiO₂ photocatalysts were prepared. One was synthesized by mixing thiourea with Ti tetraisopropoxide in a molar ratio of 1:2 during mesostructure formation using dodecylamine.⁸ The S content in the sample after template removal and evacuation at 373 K was 1.7 wt %. The obtained catalysts were denoted SN-doped mesoporous TiO₂. Another was synthesized via CVD under 101 kPa of hydrogen sulfide with mesoporous TiO₂⁸ separately synthesized using dodecylamine. The S contents in the samples were 0.48 and 0.77 wt % after CVD up to 583 and 623 K, respectively. Obtained catalysts were denoted as CVD-S-doped mesoporous TiO₂-583 or -623.

S K-edge XAFS spectra were measured at 290 K at the Photon Factory in High-Energy Accelerator Research Organization on beamline 9A (Proposal No. 2007G576). A Si(111) double crystal monochromator was fully tuned. Except for the S content evaluation in the sample based on the edge jump value in transmission mode, spectra were measured in fluorescence detection mode. A 1.4-mg portion of sample powder was ground as fine as possible and mounted on tape. The maximum of the first pre-edge feature in the spectrum of Na₂S₂O₃·5H₂O was assigned as 2472.02 eV.⁹

The S K-edge XANES spectra were theoretically generated using ab initio calculation code FEFF 8.4¹⁰ operated in self-con-

sistent field and fully multiple scattering modes. The exchange-correlation potential of the Dirac–Hara and Hedin–Lundqvist imaginary part was chosen and corrected by adding a constant shift of –2.5 eV to the Fermi level. The energy of the theoretically generated spectrum was shifted by +2.6 eV to compare to the experimental data.

Twin peaks appeared at 2470.0 and 2471.9 eV for TiS₂ (Figure 1A-d). The energy difference between S3p and Ti3d is ca. 5 eV¹¹ and the energy levels interact in TiS₂ (Scheme 1a). The twin peaks were assigned to transition to $(1 - \alpha^2)^{1/2}|\text{Ti}3d > -\alpha|\text{S}3p > (\equiv\Psi)$ levels. The intensity of this transition is proportional to the S3p character α^2 mixed into the wave function Ψ .^{9,12}

Peak energies for S K post-edge spectrum for fresh SN-doped mesoporous TiO₂ (Figure 1A-a) were 2481.8(s), 2488.5(w),

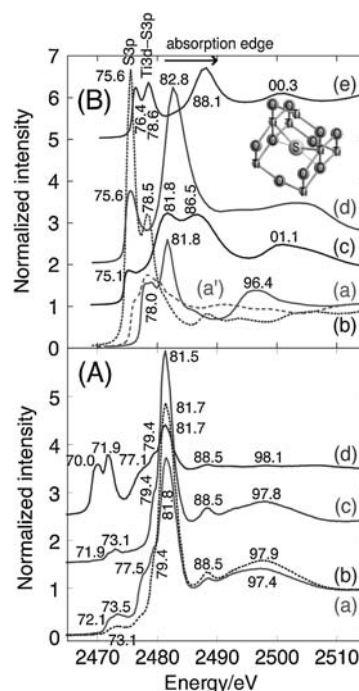
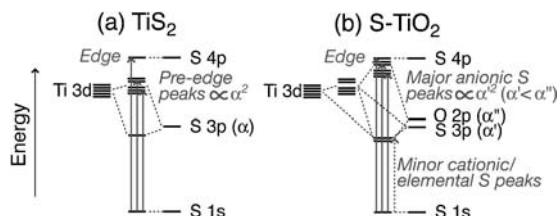


Figure 1. (A) Normalized S K-edge XANES spectra for SN-doped mesoporous TiO₂ before (a) and after ethanol oxidation under visible light (b), CVD-S-doped mesoporous TiO₂-623 after ethanol oxidation under visible light (c), and TiS₂ (d). (B) Theoretical S K-edge XANES spectra for S site substituting on the O atom (a) or Ti atom (b) of anatase-type TiO₂ or on the O atom at TiO₂(001) surface (a'), S site of SO₂ adsorbed on the Ti atom (c) or O atom (d) at TiO₂(001) surface, and S site of TiS₂ (e). (Inset) S substitution model on the O atom of TiO₂.



Scheme 1. Proposed energy diagram for TiS₂ (a) and S-doped mesoporous TiO₂ (b).

and 2497.4 eV (w, br) very similar to 2481.7, 2488.5, and 2498.1 eV for TiS₂ (Figure 1A-d). In contrast, the pre-edge feature was significantly suppressed at 2472.1 (sh) and 2473.5 eV for fresh SN-doped mesoporous TiO₂ compared to twin peaks for TiS₂. After catalysis in ethanol and O₂ gas under light >420 nm,¹³ the pre-edge peak at 2473.1 eV and the shoulder peak at 2479.4 eV became even weaker (Figure 1A-b). The S K-edge XANES spectrum for CVD-S-doped mesoporous TiO₂ was essentially identical to that for SN-doped mesoporous TiO₂ both after photocatalysis (Figures 1A-b and 1A-c). Spectra for the former negligibly changed during photocatalysis.

We assumed anatase-type TiO₂^{14,15} for theoretical calculations. Doped S substituting on O or Ti of the TiO₂ matrix (substitution model) or SO₂/SO₃H adsorbed on Ti or O at the TiO₂(001) surface.

The S K-edge XANES spectrum calculated for doped S model (total 261 atoms; Figure 1B, inset) substituting on the O of TiO₂ is depicted in Figure 1B-a. The S–Ti bond distance (*R*) was 2.283 Å (coordination number *N* = 2) based on Ti K-edge EXAFS for SN-doped mesoporous TiO₂.⁸ The absorption edge peak at 2481.8 eV, shoulder peak(s) at 2478.0 eV, and broad post-edge peak at 2496.4 eV nicely reproduced Figure 1A-a. The post-edge pattern was somewhat similar to those of sulfates^{16,17} probably because two O atoms were at 2.011 Å to doped S in the substitution model due to the strain of long Ti–S bonds in TiO₂ (Figure 1B, inset). When the *R*_{S–Ti} was elongated to 2.44 Å (CVD-S-doped mesoporous TiO₂),⁸ peaks in Figure 1B-a shifted within 1.2 eV toward lower energy but the spectral pattern was similar.

In the substitution model on Ti atom (no S site relaxation considered, total 261 atoms; Figure 1B-b) and SO₂ adsorption models on Ti (*R*_{S–Ti} = 2.44 Å, total 150 atoms; Figure 1B-c) or O atom (*R*_{S–O} = 1.574 Å, total 150 atoms; Figure 1B-d), the peaks at 2475.1–2475.6 eV became more intense as the S sites became more positive (Figure 1B-c → Figure 1B-d → Figure 1B-b). This peak was also observed for SO₂-adsorbed metal cluster.⁹ Thus, weak pre-edge peaks appearing at 2471.9–2473.5 eV (Figures 1A-a–1A-c) were due to transition to S 3p of minor cationic and/or elemental S sites⁹ in S-doped mesoporous TiO₂ (Scheme 1b). The peaks at 2471.9–2473.5 eV became weaker after photocatalysis probably because cationic/elemental S species desorbed (Figures 1A-a and 1A-b).

Calculated spectra of adsorbed SO₃H either on Ti or O consisted of peaks at 2481.7 and 2504.0 eV, but the former peak was even broader than Figure 1B-d and did not match Figures 1A-a–1A-c. Intense peaks were reported to appear between 2482.4 and 2483.4 eV for Na, Mg, Al, K, Ca, Mn, Fe, and Ba sulfates^{16,18} inconsistent with 2481.5–2481.8 eV for Figures 1A-a–1A-c. Because the catalysts could be used repeatedly for photocatalysis,⁸ the substitutional S sites on the O atoms were concluded to be

photocatalytically active rather than cationic and/or elemental S sites.

The S sites substituting on the O atoms were not necessarily at the surface because the spectrum for S substituting on the O atom at the TiO₂(001) surface (*R*_{S–Ti} = 2.283 Å, *N* = 2, total 201 atoms; Figure 1B-a') did not resemble any experimental spectra.

The twin pre-edge peaks and main peak in experimental data for TiS₂ (Figure 1A-d) were nicely reproduced at 2476.4, 2478.6, and 2488.1 eV in calculated Figure 1B-e.¹⁹ However, the peaks shifted by 6.4–6.7 eV toward lower energy in the experiment. The reason for this discrepancy is not known, but limited model cluster size of TiS₂ (88 atoms) may be critical.

The twin peaks at 2470.0 and 2471.9 eV for TiS₂ due to transition to $(1 - \alpha^2)^{1/2} |Ti3d\rangle - \alpha |S3p\rangle$ (Scheme 1a) were not observed for S-doped TiO₂ mostly because latter Ti3d antibonding levels consist of greater O2p character than S3p (S contents in catalysts: 0.48–1.7 wt %). Smaller S3p character α'^2 in the antibonding levels led to the pre-edge peaks weaker. Additionally, the interaction between Ti3d and O2p and S3p may destabilize the antibonding levels more in S-doped TiO₂ near to S4p level (Scheme 1b) than in the case between Ti3d and S3p in TiS₂.

The authors thank financial support from the Grant-in-Aid for Scientific Research C (No. 19550134) from Mext.

References

- 1 M. R. Hoffmann, S. T. Martin, W. Choi, D. W. Bahnemann, *Chem. Rev.* **1995**, *95*, 69.
- 2 A. Fujishima, K. Honda, *Nature* **1972**, *238*, 37.
- 3 V. Heleg, I. Willner, *J. Chem. Soc., Chem. Commun.* **1994**, 2113.
- 4 M. Anpo, *Bull. Chem. Soc. Jpn.* **2004**, *77*, 1427.
- 5 Y. Izumi, K. Konishi, H. Yoshitake, *Bull. Chem. Soc. Jpn.* **2008**, *81*, 1241.
- 6 Y. Izumi, K. Konishi, T. Miyajima, H. Yoshitake, *Mater. Lett.* **2008**, *62*, 861.
- 7 Y. Izumi, K. Konishi, D. M. Obaid, T. Miyajima, H. Yoshitake, *Anal. Chem.* **2007**, *79*, 6933.
- 8 Y. Izumi, T. Itoi, S. Peng, K. Oka, Y. Shibata, *J. Phys. Chem. C* **2009**, *113*, 6706.
- 9 Y. Izumi, T. Minato, K. Aika, A. Ishiguro, T. Nakajima, Y. Wakatsuki, in *Studies in Surface Science and Catalysis*, ed. by Gaigneaux, De Vos, Grange, Jacobs, Martens, Ruiz, Poncelet, Elsevier, Amsterdam, **2002**, Vol. 143A, pp. 361–368.
- 10 A. L. Ankudinov, B. Ravel, J. J. Rehr, S. D. Conradson, *Phys. Rev. B* **1998**, *58*, 7565.
- 11 G. Aschornack, *Handbook of X-ray Data*, Springer, Berlin/Heidelberg, **2007**.
- 12 A. Dey, Y. Jiang, P. O. de Montellano, K. O. Hodgson, B. Hedman, E. I. Solomon, *J. Am. Chem. Soc.* **2009**, *131*, 7869.
- 13 D. Masihi, H. Yoshitake, Y. Izumi, *Appl. Catal., A* **2007**, *325*, 276.
- 14 D. T. Cromer, K. Herrington, *J. Am. Chem. Soc.* **1955**, *77*, 4708.
- 15 B. G. Hyde, S. Andersson, *Inorganic Crystal Structures*, John Wiley & Sons, New York, **1989**.
- 16 D. H. Kim, J. H. Kwak, J. Szanyi, S. J. Cho, C. H. F. Peden, *J. Phys. Chem. C* **2008**, *112*, 2981.
- 17 H. Dathe, A. Jentys, J. A. Lercher, *Phys. Chem. Chem. Phys.* **2005**, *7*, 1283.
- 18 J. Prietzel, J. Thieme, A. Herre, M. Salomé, D. Eichert, *Eur. J. Soil. Sci.* **2008**, *59*, 730.
- 19 Y. S. Kim, M. Mizuno, I. Tanaka, H. Adachi, *Jpn. J. Appl. Phys., Part 1* **1998**, *37*, 4878.